

Communications in Physics, Vol. 26, No. 3 (2016), pp. 261-268

DOI:10.15625/0868-3166/26/3/8053

PREPARATION OF SERS SUBSTRATES FOR THE DETECTION OF ORGANIC MOLECULES AT LOW CONCENTRATION

TRAN THI KIM CHI^{1,†}, NGUYEN THI LE², BUI THI THU HIEN¹, DANG QUOC TRUNG¹
AND NGUYEN QUANG LIEM¹

¹*Institute of Materials Science, Vietnam Academy of Science and Technology,
18 Hoang Quoc Viet, Cau Giay, Hanoi, Vietnam*

²*Cao Bang Teachers' Training College, De Tham, Cao Bang, Vietnam*

[†]*E-mail: chittk@ims.vast.ac.vn*

Received 04 April 2016

Accepted for publication 10 August 2016

Abstract. *We present the preparation of surface enhanced Raman spectroscopy (SERS) substrates by depositing silver nanoparticles (Ag NPs) onto the top of 1040 nm pores of porous silicon template produced by hydrofluoric acid (HF) etching. The influences of the anodizing current density on the pore size were systematically investigated. The structural and textural characterization of the as-prepared SERS substrates were characterised by scanning electron microscope (SEM), X-ray diffraction (XRD), and Raman spectroscopy. The SERS activity was studied by Raman scattering spectra of Malachite Green (MG) molecules in water at room temperature. The SERS results showed an enhancement (20 times) by coupling of MG molecules with a localized surface plasmon resonance of Ag NPs. The limit of detection of MG molecules was determined to be 10^{-7} M.*

Keywords: SERS, chemical etching, Raman, malachite green.

Classification numbers: 33.20.Fb, 73.20.Mf.

I. INTRODUCTION

Surface-Enhanced Raman Spectroscopy (SERS) is a surface-sensitive technique that enhances the Raman scattering signal of analyte molecules adsorbed on rough metal surfaces. This enhancement factor is often observed 10^4 – 10^6 , and can be as high as 10^8 to 10^{14} for some systems [1–4]. Therefore, SERS is considered as an effective technique for chemical and bio-analytical detection [2, 3]. The enhanced Raman scattering can be explained in terms of electromagnetic and chemical mechanisms in the presence of metallic nanostructures such as silver (Ag), gold (Au), copper (Cu), and aluminum (Al) nanostructures [1–9]. Most accredited theories prove

that the electromagnetic mechanism is mainly responsible for the enhancement of Raman scattering due to the plasmon resonance created on surface of the nanostructured metal systems [5]. The plasmon resonance of Ag and Au colloidal nanoparticles (NPs) occurs in the visual wavelength range, therefore, they are the most widely used materials in the preparation of SERS substrates [2, 5, 6, 10–12]. Besides, metal films with periodic structure evaporated on solid substrates exhibit controllable, reproducible and high surface-enhancement [13–17]. Recently, the utilization of templates with periodic porous structure for deposition of Ag or Au NPs is a promising approach to fabricate SERS substrate for regarding to the improvement of SERS efficiency [6].

In this work, we report the preparation of SERS substrates and the study of Raman scattering spectra of Malachite Green (MG) adsorbed on as-prepared substrate. These SERS substrates were prepared by the deposition of Ag NPs onto the porous silicon wafer which was treated by a chemical etching with hydrofluoric acid. The impact of the anodizing current density and the etching time on the pore size as well as the time of the Ag NPs deposition were studied. The SERS efficiency of prepared SERS substrates was estimated for MG molecules.

II. EXPERIMENT

Chemicals and Characterization

- Silicon (Si) wafer (single side polished), (100) orientation, p-type, resistivity (0.01–0.018 Ωcm) were purchased from Wako (Japan, LotNo. G124-017J).

- Hydrofluoric acid (HF), silver nitrate (AgNO₃), Malachite Green (MG) were purchased from Xilong Chemical (China).

- The morphology of fabricated SERS active substrates was studied by Field Emission Scanning Electron Microscope - FE-SEM (S-4800, Hitachi, Japan,). The X-ray diffraction (XRD) patterns were recorded on a D8 (Bruker) using monochromatic CuK_α radiation ($\lambda = 1.53\text{\AA}$).

- Raman spectra of samples were recorded using a commercial (Jobin-Yvon LabRam) and home-made micro-Raman system (Horiba iHR550 high-resolution spectrometer equipped with a Hamamatsu cooled CCD and 532-nm laser as the excitation source).

Preparation of SERS substrates

SERS substrates were fabricated by two main steps: HF etching of p-type (100)-oriented Si wafer and deposition of Ag NPs onto the porous silicon.

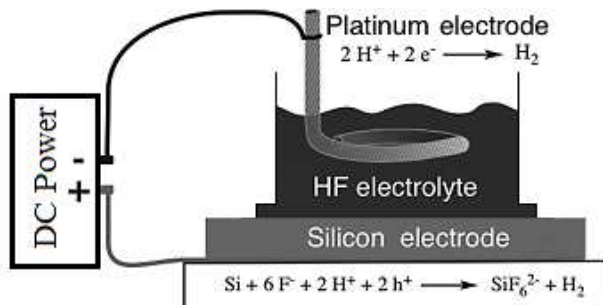


Fig. 1. Schematic of an electrochemical cell for producing porous Si wafer.

- *HF etching of (100)-oriented Si wafer* to produce the nano porous silicon template was carry out according to the reported procedures [15–17] with some modifications in anodizing current density, etching time, and silicon wafer. The roughness side of Si wafer was coated by a thick aluminum layer (100 nm) which prepared by sputtering and annealing at 450 °C for 120 minutes to obtain the Ohmic contact. The aluminum coated Si wafer was then used as a working electrode of an electrochemical cell with HF as electrolyte (Fig. 1). In this case, the working electrode acts as an anode, where an oxidation reaction takes place at its surface. The cathode electrode is platinum. The formation of porous structure is the results of the oxidation reaction at Si wafer surface. In the present work, a Teflon electrochemical cell was designed according to our etching conditions. This cell was filled with 10 mL of etching solution consisting of 48% HF and ethanol. A silicon (Si) wafer (1 cm² in area) and a Platinum (Pt) grid (2 cm in diameter) were used as the cathode and anode, respectively. The anodizing current density was changed from 25 to 150 mA.cm⁻² and the etching time was fixed as 5 s.

- *Deposition of Ag NPs* into nanopores of porous silicon wafer. This process was carried out using a simple chemical method in that the porous silicon wafer was embedded in a mixture solution of 0.1 M HF and AgNO₃ with different concentrations. Deposition time was varied between 10 and 20 minutes depending on the desired size of Ag NPs and the size of silicon wafer pores. After fabrication and thorough washing, the SERS substrates were stored in deionised water for further use.

III. RESULTS AND DISCUSSION

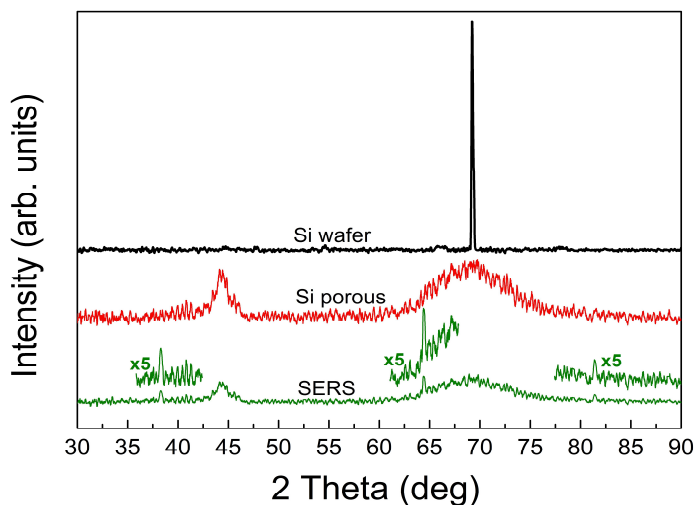


Fig. 2. XRD patterns of a (100)-oriented Si wafer (top), as-prepared porous silicon (middle) and SERS substrate (bottom). The XRD peaks of Ag NPs were magnified by factor of 5.

Figure 2 shows the XRD patterns of the (100)-oriented Si wafer before and after HF etching, and of the SERS substrate prepared at anodizing current density of 100 mA.cm⁻² and 10 minutes

of Ag NPs depositing time. It is clearly seen that silicon wafer with (100) crystalline facet shows a peak at $2\theta = 69.26^\circ$, porous silicon shows a additional peak at $2\theta = 44.28^\circ$. For porous silicon, the X-ray diffraction peak around $2\theta = 69.26^\circ$ is broadened compared to that of the crystalline silicon because of its porous nanostructures. The presence of Ag NPs on the surface of the porous silicon substrate was proved by the X-ray diffraction peaks at $2\theta = 38.32^\circ$, 64.45° , and 81.46° . The X-ray diffraction peaks of Ag NPs are weak compared to those of silicon because the amount of Ag NPs is very small compared with silicon.

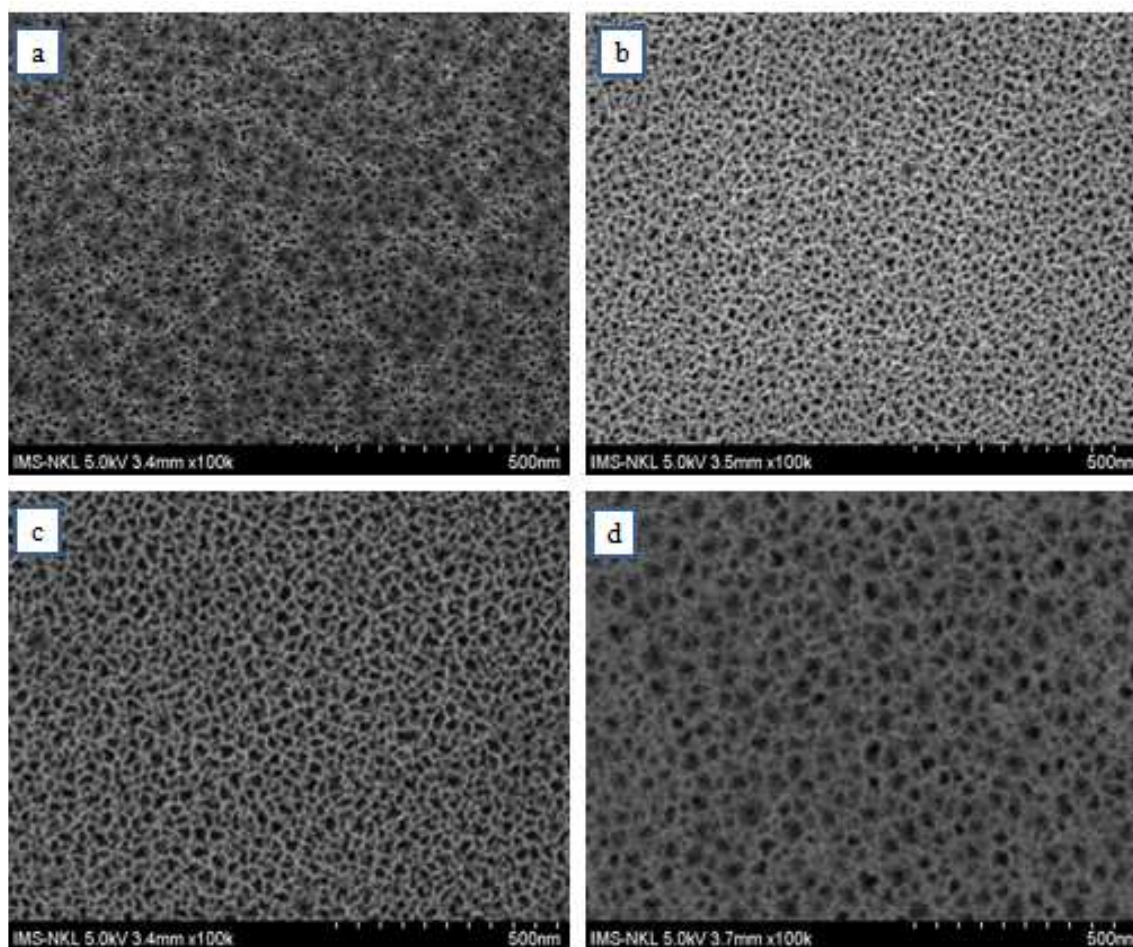


Fig. 3. SEM images of porous silicon samples prepared by HF etching of (100)-oriented Si wafer at different anodizing current densities: (a) $25 \text{ mA}\cdot\text{cm}^{-2}$, (b) $50 \text{ mA}\cdot\text{cm}^{-2}$, (c) $100 \text{ mA}\cdot\text{cm}^{-2}$, and (d) $150 \text{ mA}\cdot\text{cm}^{-2}$ for 5 seconds etching time.

Figure 3 shows the SEM images of porous silicon samples obtained by HF etching with different anodizing current densities. The results show that the uniform porous silicon structure was formed under all applied anodizing current densities. The pore size is a linear function of the anodizing current density: 10 nm, 15 nm, 30 nm and 40 nm corresponding to the anodizing current

densities as $25 \text{ mA}\cdot\text{cm}^{-2}$, $50 \text{ mA}\cdot\text{cm}^{-2}$, $100 \text{ mA}\cdot\text{cm}^{-2}$ and $150 \text{ mA}\cdot\text{cm}^{-2}$ (Fig. 3). However, the sample having the most homogenous pores was obtained under $100 \text{ mA}\cdot\text{cm}^{-2}$ anodizing current density. Therefore, this current density was used in the next depositions. In Fig. 4, it is clear that the Ag NPs are formed in the pores at 1 mM AgNO_3 . The AgNO_3 becomes clusters on the top of pore when the AgNO_3 concentration increases (2 and 3 mM). The clusters shrink to spheroid NPs at 5 mM AgNO_3 . The Ag NPs were deposited on the porous silicon by in situ reduction of AgNO_3 in acidic media (0.1 M HF) for 10 minutes. The obtained substrates were annealed at 500° for 30 minutes in ambient.

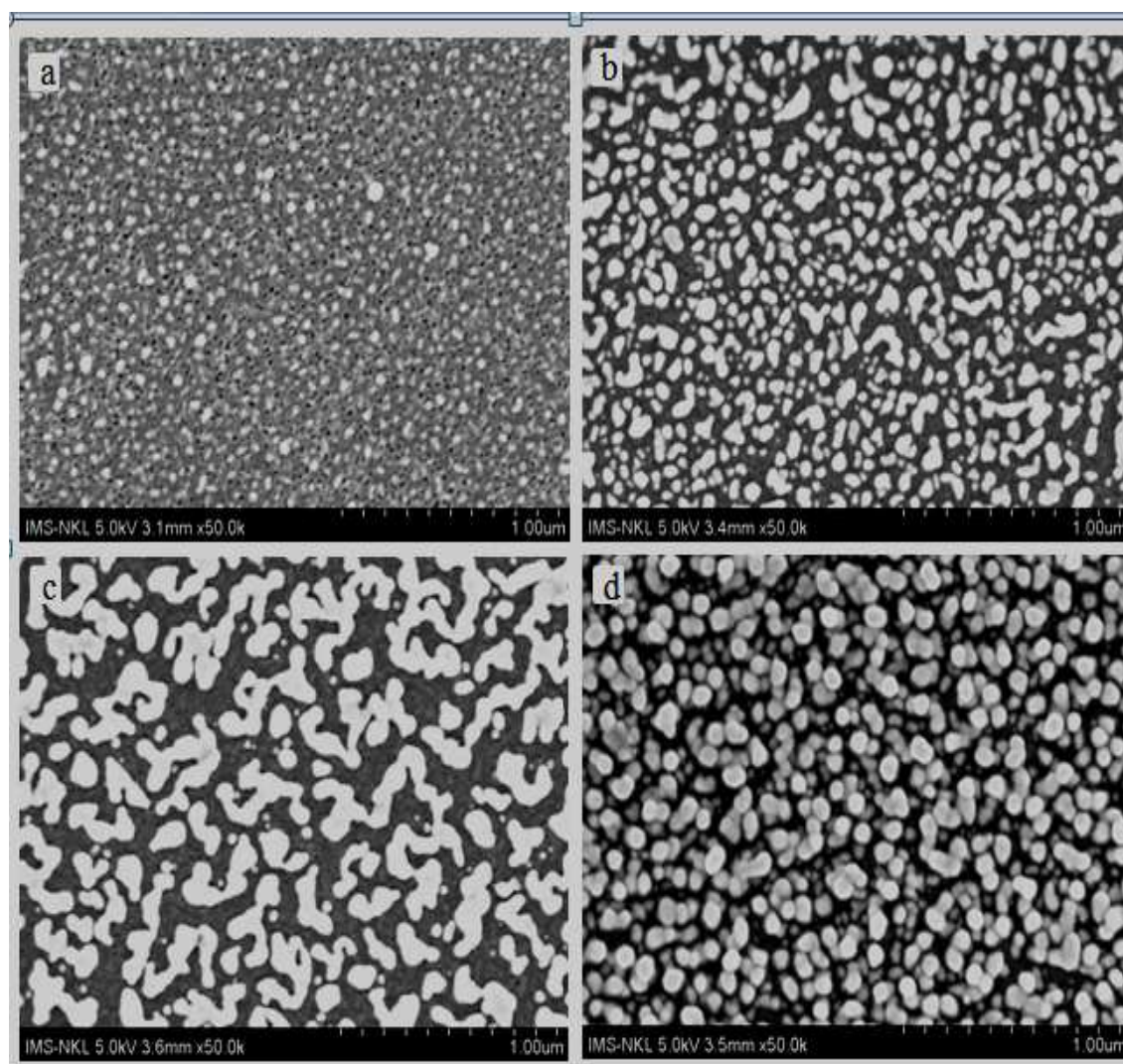


Fig. 4. SEM images of fabricated SERS substrates at different AgNO_3 concentrations: (a) 1 mM , (b) 2 mM (c) 3 mM , and (d) 5 mM AgNO_3 . Deposition time is 10 minutes.

The SERS effect of the fabricated substrates was studied by the Raman spectra of Malachite Green (MG) in water. 10 μL of aqueous MG solutions with different concentrations were dropped onto the as-prepared SERS substrates and dried before measurement. The spreading area is $\sim 1 \times 1 \text{ cm}^2$.

Figure 5 shows the Raman spectra of MG solution dropped on a Si wafer and the as-prepared SERS substrate. The characteristic Raman peaks of MG were clearly observed in the high-frequency region [18, 19]. Namely, the strong Raman band belonging to N–C bonding and C–C stretching vibrations was observed at 1617 cm^{-1} . The bands at 1171 cm^{-1} and 1294 cm^{-1} can be assigned to the aromatic C–H in-plane bending vibrations; and 1366 cm^{-1} can be ascribed to the N–C stretching vibration coupled with the C–C and C–H in-plane motions at 1394 cm^{-1} . The band appeared at 914 cm^{-1} can be attributed to the ring skeletal radial vibration. Compared to the spectrum of MG dropped onto Si wafer, a remarkable increase in intensity of the active Raman peaks (20 times) proves the plasmon resonance-assisted effect exhibited by the presence of Ag NPs

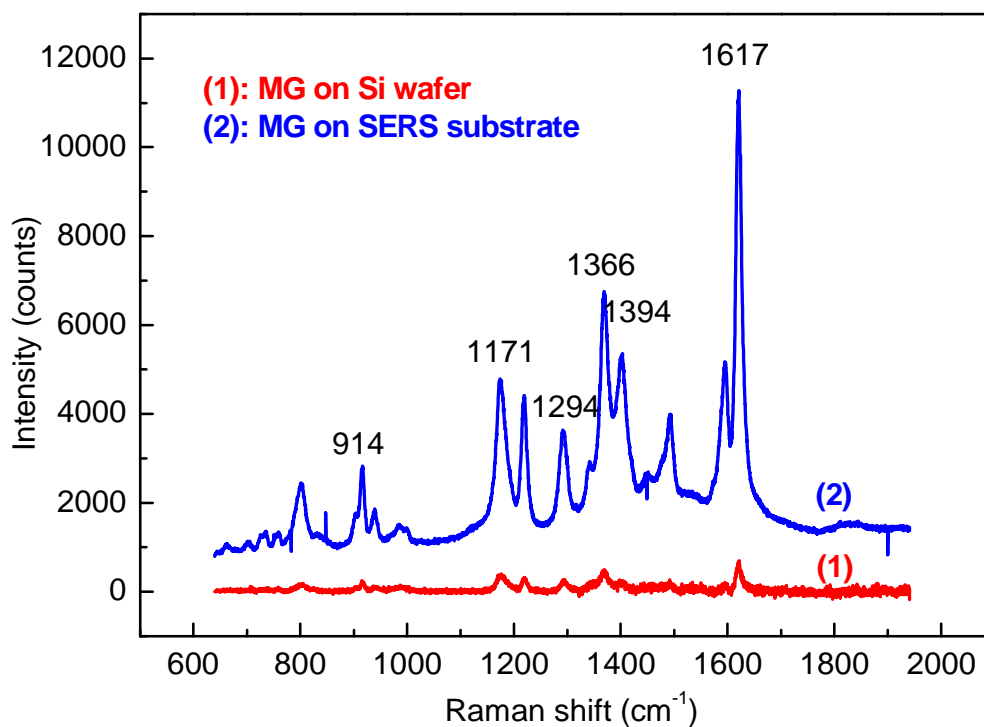


Fig. 5. Raman spectra of Malachite Green of concentration: $2 \times 10^{-5} \text{ M}$ dropped onto (1) Si wafer and (2) SERS substrate prepared at 2 mM AgNO_3 .

Figure 6 shows the Raman spectra of MG molecules at 10^{-5} , 10^{-6} and 10^{-7} M dropped onto the SERS substrate of 2 mM AgNO_3 deposition. It is clearly seen that the Raman scattering signal is increased with the MG concentration and SERS substrate can be used to detect MG molecules at concentration as low as 10^{-7} M .

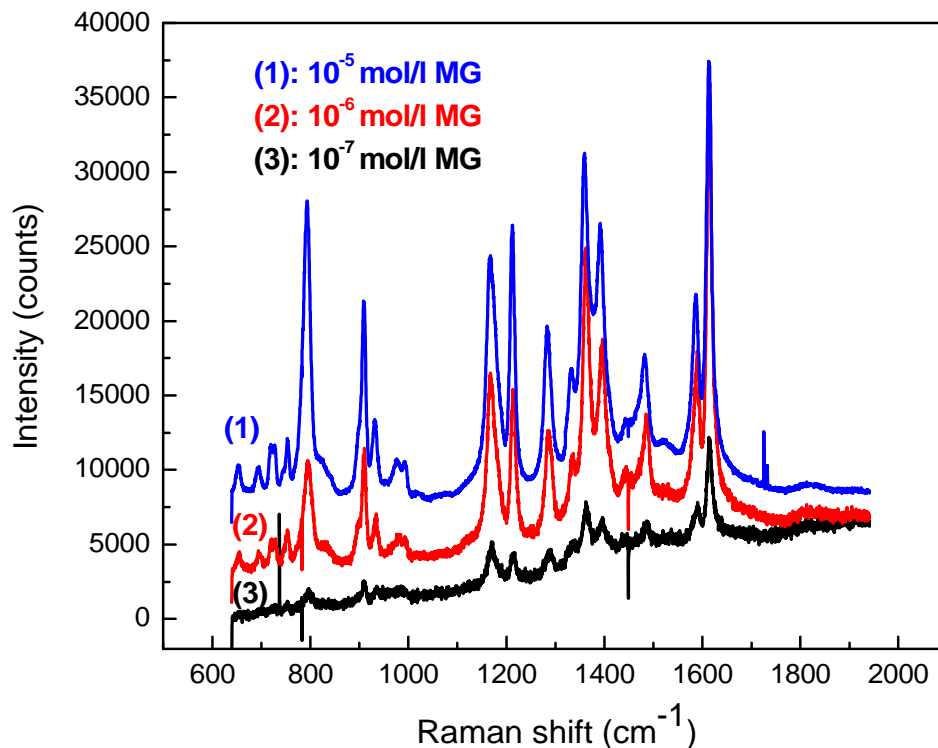


Fig. 6. Raman spectra of MG with various concentrations (1) 10^{-5} M (2) 10^{-6} M, and (3) 10^{-7} M dropped onto the SERS substrate of 2 mM AgNO_3 deposition.

IV. CONCLUSION

The SERS substrates were successfully fabricated by deposition of Ag NPs onto the porous silicon template by in situ reduction of AgNO_3 in 0.1 M HF. The porous silicon structure was formed by anodization HF etching the low resistivity p-type (100) silicon wafers. The pore size increases with increasing the anodizing current density. Especially, the silicon template with uniform pore size distribution was obtained at the anodizing current density of $100 \text{ mA}\cdot\text{cm}^{-2}$. The fabricated SERS substrates were used to detect MG molecules and the limit of detection was determined to be 10^{-7} M.

ACKNOWLEDGMENTS

This work was supported by Ministry of Science and Technology (e-ASIA Project No.33/2013/HD-NDT) and Vietnam Academy of Science and Technology (VAST.ĐL.06/13-14). We thank National Key Laboratory for Electronic Materials and Devices (VAST/IMS) for the use of facilities.

REFERENCES

- [1] U. K. Sur and J. Chowdhury, *Curr. Sci* **105** (2013) 923.
- [2] B. Sharma, R. R. Frontiera, A.-I. Henry, E. Ringe and R. P. Van Duyne, *Materials Today* **15** (2012) 16.
- [3] M. Fan, G. F. Andrade and A. G. Brolo, *Anal. Chim. Acta* **693** (2011) 7.
- [4] S. Daniel, *Improved performance of reduced silver substrates in surface enhanced raman scattering*, Master's thesis, University of Eastern Finland, 2013.
- [5] G. M. Herrera, A. C. Padilla and S. P. Hernandez-Rivera, *Nanomaterials* **3** (2013) 158.
- [6] L. A. Dick, A. J. Haes and R. P. Van Duyne, *J. Phys. Chem. B* **104** (2000) 11752.
- [7] A. M. Michaels, J. Jiang and L. Brus, *J. Phys. Chem. B* **104** (2000) 11965.
- [8] S.-P. Chen, C. M. Hosten, A. Vivoni, R. L. Birke and J. R. Lombardi, *Langmuir* **18** (2002) 9888.
- [9] J. R. Lombardi, R. L. Birke, T. Lu and J. Xu, *J. Chem. Phys.* **84** (1986) 4174.
- [10] T. Q. N. Luong, T. A. Cao and T. C. Dao, *Adv. Nat. Sci.: Nanosci. Nanotechnol.* **4** (2013) 015018.
- [11] T. C. Dao, T. Q. N. Luong, T. A. Cao, N. H. Nguyen, N. M. Kieu, T. T. Luong and V. V. Le, *Adv. Nat. Sci.: Nanosci. Nanotechnol.* **6** (2015) 035012.
- [12] T. C. Dao, T. Q. N. Luong, T. A. Cao, N. M. Kieu et al., *Adv. Nat. Sci.: Nanosci. Nanotechnol.* **7** (2016) 015007.
- [13] C. L. Haynes, A. D. McFarland, M. T. Smith, J. C. Hulteen and R. P. Van Duyne, *J. Phys. Chem. B* **106** (2002) 1898.
- [14] Y. Jiao, D. S. Koktysh, N. Phambu and S. M. Weiss, *Applied Physics Letters* **97** (2010) 153125.
- [15] H. Lin, J. Mock, D. Smith, T. Gao and M. J. Sailor, *J. Phys. Chem. B* **108** (2004) 11654.
- [16] F. Giorgis, E. Descrovi, A. Chiodoni, E. Froner, M. Scarpa, A. Venturello and F. Geobaldo, *Appl. Surf. Sci.* **254** (2008) 7494.
- [17] J. N. G. Bugayong, *Electrochemical etching of isolated structures in p-type silicon*, Ph.D. thesis, University of the Philippines at Los Baños, 2011.
- [18] B. Pettinger, B. Ren, G. Picardi, R. Schuster and G. Ertl, *J. Raman Spectrosc.* **36** (2005) 541.
- [19] Y. Zhao, Y. Tian, P. Ma, A. Yu, H. Zhang and Y. Chen, *Anal. Methods* **7** (2015) 8116.